Conformational Transitions of an Unmodified tRNA: Implications for RNA Folding†

Emily J. Maglott,‡ Sanmitra S. Deo,‡ Anna Przykorska,§ and Gary D. Glick*,‡

Department of Chemistry, University of Michigan, Ann Arbor, Michigan 48109-1055, and Institute of Biochemistry and Biophysics, Polish Academy of Sciences, Pawinskiego 5a, 02 106 Warsaw, Poland

Received July 17, 1998

ABSTRACT: Unmodified tRNAs are powerful systems to study the effects of posttranscriptional modifications and site-directed mutations on both the structure and function of these ribonucleic acids. To define the general limitations of synthetic constructs as models for native tRNAs, it is necessary to elucidate the conformational states of unmodified tRNAs as a function of solution conditions. Here we report the conformational properties of unmodified yeast $tRNA^{Phe}$ as a function of ionic strength, [Mg^{2+}], and temperature using a combination of spectroscopic measurements along with chemical and enzymatic probes. We find that in low [Na^{+}] buffer at low temperature, native yeast $tRNA^{Phe}$ adopts tertiary structure in the absence of Mg^{2+}. By contrast, tertiary folding of unmodified yeast $tRNA^{Phe}$ has an absolute requirement for Mg^{2+}. Below the melting temperature of the cloverleaf, unmodified yeast $tRNA^{Phe}$ exists in a Mg^{2+}-dependent equilibrium between secondary and tertiary structure. Taken together, our findings suggest that although the tertiary structures of tRNAs are broadly comparable, the intrinsic stability of the tertiary fold, the conformational properties of intermediate states, and the stability of intermediate states can differ significantly between tRNA sequences. Thus, the use of unmodified tRNAs as models for native constructs can have significant limitations. Broad conclusions regarding "tRNA folding" as a whole must be viewed cautiously, particularly in cases where structural changes occur, such as during protein synthesis.

One of the features that distinguishes transfer RNAs from other cellular RNAs is the diversity and prevalence of posttranscriptionally modified bases (*1*). These modifications range from simple methylation to hypermodifications such as wybutosine and queuosine. In some cases, base modifications serve as identity elements for the interactions of tRNA with other macromolecules (*2*), whereas others are thought to help stabilize both the tertiary folded structure and the cloverleaf secondary structure (*3*−*6*). However, the way in which posttranscriptional modifications exert their stabilizing effects on both secondary and tertiary structure is not fully understood.

Probing the role of the modified nucleosides in tRNA has been facilitated by both solid-phase synthesis and in vitro transcription methodology, which allow the synthesis of tRNAs lacking base modifications (*6*, *7*). The influence of modified nucleosides on both structure and function can be determined from a comparison of the properties of the "unmodified" tRNAs with the corresponding native tRNAs. Unmodified tRNAs have mostly been used to study interactions with the translational machinery. They often retain the ability to bind to their cognate synthetase (*8*−*15*), and are functional in interactions with both elongation factor Tu (*16*) and enzymes that introduce posttranscriptional modification (*17*). The competence of unmodified tRNAs in these processes suggests that the gross structures of unmodified and native tRNAs are similar.

The structures of five unmodified tRNAs (yeast, Phe and Asp; *Escherichia coli*, Val and Gln; human mitochondrial, Lys) have been probed either by chemical and enzymatic footprinting (*3*, *18*−*22*), or by NMR spectroscopy (*5*, *23*), or by X-ray crystallography (*24*). With the exception of human mitochondrial $tRNA^{Lys}$ (*3*), these other unmodified tRNAs fold properly in the presence of Mg^{2+}. However, thermal denaturation studies indicate that the unmodified tRNAs generally require higher [Mg^{2+}] to achieve thermal stabilities comparable to the corresponding native sequences (*4*, *6*, *22*, *24*). Collectively, these results suggest that modified bases are not essential for tertiary folding, but rather that they modulate the stability of tertiary structure (*23*).

Since the posttranscriptional modifications have roles in both structure and function, delineating the conformational states of unmodified (and partially modified) tRNAs as a function of solution conditions is necessary to fully understand the structural and energetic roles of the modified bases. This information is also necessary to define the limitations of synthetic tRNAs as models for the naturally occurring systems. Here, we report the conformational properties of unmodified yeast $tRNA^{Phe}$ [1] investigated under conditions of varying ionic strength, [Mg^{2+}], and temperature using a combination of spectroscopic techniques along with chemical and enzymatic probes. In contrast to native yeast $tRNA^{Phe}$,

† Supported by NIH Grant GM-52168 to G.D.G. A.P. acknowledges funding from State Committee for Scientific Research (KBN) Grant 6 P04A 063 10. E.J.M. and S.S.D. acknowledge partial support from NIH Molecular Biophysics and Chemistry−Biology Interface Training Programs, respectively.

* Address correspondence to this author. Phone: (734) 764-4548. FAX: (734) 764-8815. E-mail: gglick@umich.edu.

‡ University of Michigan.

§ Polish Academy of Sciences.

10.1021/bi981722u CCC: $15.00
Published on Web 10/29/1998

we find that at temperatures below the denaturation temperature of the cloverleaf secondary structure, unmodified yeast $tRNA^{Phe}$ exists in a Mg^{2+}-dependent equilibrium between secondary and tertiary structure. While the $[Mg^{2+}]$ required for tertiary folding differs for native and unmodified yeast $tRNA^{Phe}$, the binding of Mg^{2+} to both molecules appears similar. Collectively, our results suggest that while the conformations of folded tRNAs may be comparable, the intrinsic stability of the tertiary fold and the structures and stabilities of other conformational states may differ. Therefore, a single conformation-phase diagram is insufficient to explain all "tRNA folding".

MATERIALS AND METHODS

Unmodified yeast $tRNA^{Phe}$ was prepared by either in vitro transcription (*25*) or chemical synthesis using A^{Pac} (or A^{Bz}), C^{Bz}, G^{Pac}, and U β-cyanoethyldiisopropyl phosphoramidites with the 2′-hydroxyl groups protected as *tert*-butyldimethylsilyl ethers (PerSeptive Biosystems, Biogenex) on an Expedite 8909 synthesizer. Chemically synthesized tRNA was deprotected, desilylated, and purified as previously described (*26*, *27*) and is indistinguishable from the in vitro transcript in a charging assay (*7*). The oligonucleotide used in primer extension experiments (5′-TGGTGCGAATTCT-GTG) was synthesized using standard phosphoramidite chemistry, purified using an oligonucleotide purification cartridge (Applied Biosystems, Foster City, CA), and 5′-^{32}P end-labeled as previously described (*26*).

Nuclease S1 was obtained from Boehringer Mannheim (Indianapolis, IN), RNase T2 grade V from *Aspergillus oryzae* was obtained from Sigma Chemical Co. (St. Louis, MO), and RNase V1 was obtained from Pharmacia (Piscataway, NJ). Rn nuclease I was isolated as previously described (*28*). SuperScript II was obtained from Life Technologies (Gaithersburg, MD).

Structure Mapping. 3′-^{32}P labeled tRNA was prepared according to the method of England and Uhlenbeck (*29*). 5′-^{32}P labeled tRNA was prepared as previously described (*26*). For mapping experiments, labeled tRNA samples were dissolved in buffer (4 μL, 10 mM NaCac, 90 mM NaCl, pH 6.8, varying amounts of $MgCl_2$), heated to 70 °C for 2 min, and then cooled to 35 °C at 3 °C/min. Samples were further cooled to 15 °C at 10 °C/min and equilibrated at 15 °C for 2 min. The temperature was adjusted to the final incubation temperature, and the solution was equilibrated for 3 min. Enzyme solutions, diluted as necessary with the reaction buffer (0.04 unit/μL Rn nuclease I; 0.2 unit/μL nuclease S1; 0.0024 unit/μL RNase T2; 0.72 unit/μL RNase V1), were added, and the tRNA/enzyme solution was incubated for 8 min. The reactions were quenched with 1 mg of brewer's yeast tRNA and 7.4 M urea, 50 mM EDTA (6 μL). All footprinting experiments were analyzed on denaturing gels [15% polyacrylamide, 29:1 acrylamide:bis(acrylamide), 8 M urea; 31.0 cm × 38.5 cm × 0.4 mm] electrophoresed in TBE buffer (90 mM Tris·borate, 2 mM EDTA, pH 8.3). Product bands were quantified using a Molecular Dynamics phosphorimager and ImageQuant software v 1.2 (Molecular Dynamics).

Rates of Pb(II) autocleavage were measured as described by Han and Dervan (*18*), and ultraviolet cross-link formation was performed using the method of Behlen et al. (*20*). Chemical modification experiments were conducted essentially following the protocol of Peattie and Gilbert (*30*) using 3′-^{32}P labeled tRNA. Reactions (100 μL) were conducted in 10 mM NaCac, 90 mM NaCl, pH 6.8, with varying amounts of $MgCl_2$ without added carrier. DMS and DEPC were added to final concentrations of 53 mM and 35 mM, respectively. All reactions were quenched by the addition of NaOAc (25 μL, 1.5 M) and methylated carrier tRNA (10 μg) (*31*) followed by two EtOH precipitations. Aniline acetate cleavage was performed using the conditions of Zueva and co-workers (*31*). tRNA samples were heat denatured (85 °C, 2 min) and analyzed as described above.

Primer extension analysis of chemical modification by CMCT, DEPC, and DMS was conducted essentially as described by Banerjee et al. (*32*) except that glycogen was used as a coprecipitant. Primer extension reactions contained tRNA (2.4 ng), 5′-^{32}P-16mer complementary to the 3′ end of $tRNA^{Phe}$ (2.6 ng), DMSO (1 mM), and SuperScript II (200 units, MMLV-RT, RNase H^-).

Native Gel Electrophoresis. An aliquot of an aqueous solution of each ^{32}P end-labeled tRNA (7500 cpm) was concentrated in vacuo and dissolved in either 5× NaCac buffer (1 μL, 50 mM NaCac, 450 mM NaCl, pH 6.8) or 5× NaCac/Mg buffer (1 μL, 50 mM NaCac, 450 mM NaCl, 25 mM $MgCl_2$, pH 6.8) and H_2O (4 μL). The samples were heated and annealed as described above. Sucrose loading buffer (5 μL, 25% w/v) was added, and each sample was loaded onto a native gel [12% polyacrylamide, 29:1 acrylamide:bis(acrylamide); 14 cm × 16 cm × 0.8 mm] which had been equilibrated at RT for 1 h after polymerization. The samples were electrophoresed at constant voltage (300 V) for 6 h in either 1× NaCac buffer or 1× NaCac/Mg buffer at 20 °C using a Hoefer SE600 electrophoresis apparatus attached to a recirculating water bath, until the xylene cyanole tracking dye (in a blank lane) had migrated 13.5 cm.

UV Thermal Denaturation. UV spectra were measured on a Cary 3 spectrophotometer equipped with a Varian Peltier. tRNA samples were prepared by dialysis against the requisite buffer. The buffers used were either 10 mM NaCac, pH 6.8, or 5 mM Na_2HPO_4, pH 6.8, with the final $[Na^+]$ achieved by addition of NaCl. Thermal denaturation curves obtained with each buffer were identical. Aliquots of dialyzed tRNA were diluted with the same degassed buffer to a final volume of 1 mL with a final [tRNA] = 0.5 μM in 10-mm-long self-masking cuvettes. Samples were heat-denatured at 85 °C for 1 min and then cooled to 5 °C at a cooling rate of 3 °C/min. The tRNA samples were equilibrated at 5 °C for 30 min and then heated at a rate of 0.5 °C/min while monitoring the absorbance.

Circular Dichroism. Measurements were conducted on an AVIV 62DS spectrophotometer equipped with a thermoprogrammable Peltier with a step size of 1 nm, a bandwidth of 1.5 nm, and a signal averaging time of 1.0 s. Samples of unmodified yeast $tRNA^{Phe}$ were dissolved in 10 mM NaCac, 90 mM NaCl, pH 6.8, folded as described above, and

[1] Abbreviations: yeast $tRNA^{Phe}$, phenylalanine-specific transfer RNA from yeast; unmodified yeast $tRNA^{Phe}$, yeast $tRNA^{Phe}$ lacking post-transcriptional modifications; NaCac, sodium cacodylate; DMS, dimethyl sulfate; DEPC, diethyl pyrocarbonate; CMCT, 1-cyclohexyl-3-(2-morpholinoethyl)carbodiimide metho-*p*-toluenesulfonate; EDTA, ethylenediamine-*N*,*N*,*N*′,*N*′-tetraacetic acid; CDTA, *trans*-1,2-diaminocyclohexane-*N*,*N*,*N*′,*N*′-tetraacetic acid.

equilibrated at 25 °C for 10 min before acquiring the spectrum. Aliquots of Mg^{2+} (0.5 μL, 0.2 M) were added to the tRNA sample and equilibrated for 10 min between acquisition of each spectrum. Experiments with native yeast $tRNA^{Phe}$ were conducted similarly except the tRNA was dissolved in 10 mM NaCac, 22 mM NaCl, pH 6.8, folded as described above, and equilibrated at either 15 °C or 40 °C before acquiring the spectrum.

Kinetic Measurements. Rates of tertiary structure unfolding were measured using an Applied Photophysics, Ltd., Model SX18MV stopped-flow spectrophotometer. Prior to use, samples were dialyzed against buffer (10 mM NaCac, 90 mM NaCl, 5 mM $MgCl_2$, pH 6.8). The dialyzed tRNA was diluted with filtered buffer to a final concentration of 0.9 μM. Immediately prior to use, aliquots of this solution (1 mL) were heated to 70 °C for 5 min and then cooled to room temperature over 30 min to properly fold the tRNA. In a typical unfolding experiment, a solution of folded tRNA (0.9 μM) and an EDTA solution (2−35 mM, in 10 mM NaCac, total $[Na^+] = 100$ mM) were each equilibrated in the stopped-flow instrument at the desired temperature for 15 min prior to mixing. The pH of the EDTA solutions was adjusted to provide a final pH of 6.8 upon mixing. Mixing was commenced using equal volumes (50 μL) of the two solutions, and the unfolding transition was monitored at 268 nm. A minimum of seven kinetic traces were obtained at each temperature and each [EDTA]. All kinetic data obtained under a given set of conditions were averaged, and the average trace was analyzed using the Kinetic Spectrometer Workstation Software provided with the instrument. Errors to these fits were <6% of the rate. Standard deviations for the rates were calculated from exponential fits to each of the traces that were included in the average rate. To determine activation parameters, Eyring plots were constructed for each [EDTA] as described by Cole et al. (*33*).

RESULTS

Structure of Yeast $tRNA^{Phe}$ and Unmodified Yeast $tRNA^{Phe}$ at Low $[Na^+]$. Based on calorimetry and ethidium bromide binding measurements, Coutts et al. (*34*) and Privalov and Filimonov (*35*) proposed that yeast $tRNA^{Phe}$ folds properly to the canonical L-shaped tertiary structure in low-salt buffers lacking Mg^{2+}. In such low-salt buffers (e.g., 32 mM Na^+, pH 6.8), thermal denaturation of yeast $tRNA^{Phe}$ is characterized by five sequential conformational transitions. The first transition spans 15−35 °C and corresponds to conversion of the native folded tertiary structure to the cloverleaf, and the subsequent melting events that occur at higher temperatures represent denaturation of the structural units comprising the cloverleaf (*34*−*38*). Recently, however, it was suggested that native yeast $tRNA^{Phe}$ does not adopt tertiary structure in low-salt buffers lacking Mg^{2+} (*39*). Because this conclusion contradicts a body of literature and it was based on experiments using an *unmodified* yeast $tRNA^{Phe}$ analogue as a *model* of native yeast $tRNA^{Phe}$, we examined the structure of yeast $tRNA^{Phe}$ in the absence of Mg^{2+} by measuring the rate of Pb^{2+}-induced hydrolysis (*18, 21*) and ultraviolet cross-linking (*20*). Both of these assays are sensitive probes of the D-loop/T-loop interface that have been used to assess tertiary structure formation in tRNAs. To our knowledge, this investigation represents the first chemical mapping experiment conducted on yeast $tRNA^{Phe}$ under the low-salt conditions described by both Coutts et al. (*34*) and Privalov and Filimonov (*35*).

Table 1: Pb^{2+} Cleavage Rates for Yeast $tRNA^{Phe}$ and Unmodified Yeast $tRNA^{Phe}$ at 15 °C in 10 mM NaCac, 22 mM NaCl, pH 6.8[a]

$tRNA^{Phe}$	rate, $s^{-1} \times 10^4$; $-Mg^{2+}$	rate, $s^{-1} \times 10^4$; $+ Mg^{2+}$
yeast[b]	23 ± 1	21 ± 2
unmodified[c]	0.54 ± 0.01	8.0 ± 0.6

[a] As previously noted, the rate of Pb^{2+} cleavage for unmodified yeast $tRNA^{Phe}$ is slower than yeast $tRNA^{Phe}$ and has been ascribed to a less ordered tertiary structure for unmodified yeast $tRNA^{Phe}$ (*18, 21*). [b] 1 mM Mg^{2+}. [c] 5 mM Mg^{2+}.

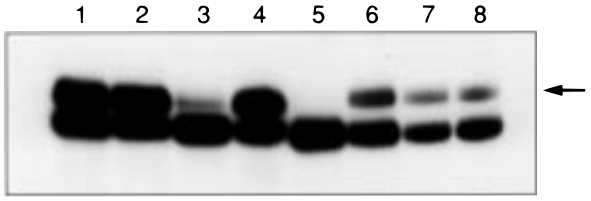

FIGURE 1: Ultraviolet cross-linking of yeast $tRNA^{Phe}$ (lanes 1−4) and unmodified yeast $tRNA^{Phe}$ (lanes 5−8) in 10 mM NaCac, 22 mM NaCl, pH 6.8. Lane 1, 15 °C; lane 2, 15 °C, 1 mM Mg^{2+}; lane 3, 40 °C; lane 4, 40 °C, 1 mM Mg^{2+}; lane 5, 15 °C; lane 6, 15 °C, 1 mM Mg^{2+}; lane 7, 15 °C, 5 mM Mg^{2+}; lane 8, 40 °C, 5 mM Mg^{2+}. The arrow indicates cross-linked tRNA.

The rate of specific Pb^{2+}-induced cleavage between residues U17 and G18 in native yeast $tRNA^{Phe}$ at 15 °C in 32 mM Na^+ buffer is identical in both the presence and absence of Mg^{2+} (Table 1). Furthermore, in both the presence and absence of Mg^{2+}, formation of an ultraviolet cross-link between residues C48 and U59 occurs to identical levels (36%, Figure 1). In the sequential unfolding pathway proposed by both Coutts et al. (*34*) and Privalov and Filimonov (*35*), tertiary structure is completely denatured above 35 °C in the absence of Mg^{2+}. Consistent with this model, only 6% cross-linking is observed in the absence of Mg^{2+} at 40 °C (which is near background), while no decrease in cross-link formation occurs in the presence of Mg^{2+} at 40 °C, where tertiary structure is stabilized and denaturation of secondary and tertiary structure is coupled (*35*). In agreement with the original proposal of both Coutts et al. (*34*) and Privalov and Filimonov (*35*), our experiments indicate that the tertiary structure of native yeast $tRNA^{Phe}$ forms in low-salt buffer in the absence of Mg^{2+}; addition of Mg^{2+} stabilizes the tRNA structure and shifts denaturation to higher temperatures.

Lead(II) cleavage and UV cross-linking experiments were also used to examine the solution structure of unmodified yeast $tRNA^{Phe}$ in a 32 mM Na^+ buffer. In the absence of Mg^{2+}, the rate of specific Pb^{2+}-induced cleavage for unmodified yeast $tRNA^{Phe}$ is 15-fold lower than the rate measured in the presence of Mg^{2+}, implying that the specific binding site for Pb^{2+} created in the tertiary structure is not formed when Mg^{2+} is not present (*21*). Furthermore, an ultraviolet cross-link between C48 and U59 is not observed in unmodified yeast $tRNA^{Phe}$ in the absence of Mg^{2+} (Figure 1), although addition of Mg^{2+} (5 mM) restores cross-link formation to a level comparable to that obtained with yeast $tRNA^{Phe}$ (31%). Taken together, these data indicate that the tertiary structure of unmodified yeast $tRNA^{Phe}$ is absent in 32 mM Na^+.

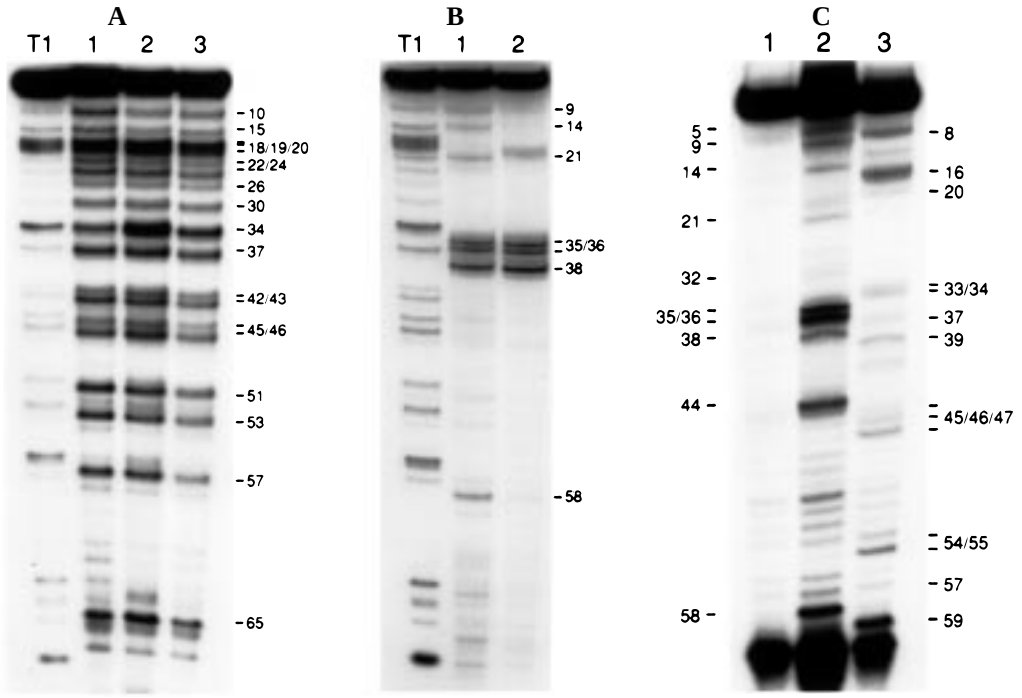

FIGURE 2: Chemical modification of [3′-^{32}P] unmodified yeast tRNA^{Phe} in 10 mM NaCac, 90 mM NaCl, pH 6.8, with varying amounts of $MgCl_2$ at 25 °C. (A) DMS analysis by strand scission: T1, denaturing RNase T1 ladder; lane 1, 0 mM Mg^{2+}; lane 2, 5 mM Mg^{2+}; lane 3, 10 mM Mg^{2+}. (B) DEPC analysis by strand scission: T1, denaturing RNase T1 ladder; lane 1, 0 mM Mg^{2+}; lane 2, 5 mM Mg^{2+}. (C) Analysis by primer extension: lane 1, control incubation without probe; lane 2, DMS; lane 3, CMCT. Modification occurs at both the N^7 (DEPC) and the N^1 (DMS) positions of all single-stranded adenosine residues. CMCT cleavage is not observed at all single-stranded guanosines because this reagent reacts more readily with U residues than G residues (*40*).

Since UV cross-link formation and Pb^{2+} cleavage only report on the structure of the hinge region, DMS footprinting experiments capable of monitoring tertiary interactions throughout the entire sequence were conducted. In the presence of 5 mM Mg^{2+}, unmodified yeast tRNA^{Phe} is protected from reaction with DMS (which alkylates at the N^7-position of guanosine) at residue G22, which the crystal structure of yeast tRNA^{Phe} predicts should be involved in a tertiary interaction (Figure 2). Several residues in the D-stem and loop (G10, G15, G22, G26) as well as the variable loop (G42, G43, G45) and the T-stem (G51, G53, G65) are also protected from modification. Each of these residues is also protected in the folded structure of native yeast tRNA^{Phe} (*30*, *41*). The similarity of the footprinting patterns of unmodified and native yeast tRNA^{Phe} supports the conclusion that the tertiary structure of unmodified yeast tRNA^{Phe} forms in 100 mM Na^+, 5 mM Mg^{2+}, pH 6.8, in agreement with earlier NMR results reported by Hall et al. (*23*).

To determine if monovalent ions alone can stabilize the tertiary structure of unmodified yeast tRNA^{Phe} as in the case of native yeast tRNA^{Phe}, tertiary structure formation was examined in buffers containing varying amounts of salt. Because the chemistry of UV cross-link formation is independent of buffer, tertiary structure formation was assessed by UV cross-linking over monovalent ion concentrations ranging from 50 mM to 2 M at 20 °C. It should be noted that Pb^{2+} hydrolysis could not be used for these experiments since we have observed that Pb^{2+} cleavage of tRNA is inhibited at salt concentrations >250 mM. Even at 2 M monovalent ion, UV cross-link formation is significantly lower than in the presence of Mg^{2+} (Figure 3). This observation suggests that at high salt in the absence of Mg^{2+} either native tertiary structure does not form or only a population of molecules folds properly. Thus, Mg^{2+} ions are essential to maintain the folded structure of unmodified yeast tRNA^{Phe}.

In summary, these experiments highlight an important difference between native yeast tRNA^{Phe} and unmodified yeast tRNA^{Phe}. Although the tertiary structure of yeast tRNA^{Phe} forms under a variety of conditions, tertiary structure formation in unmodified yeast tRNA^{Phe} requires Mg^{2+}. Based on these results, we conclude that at least for yeast tRNA^{Phe}, the unmodified tRNA is not an appropriate model for the native tRNA in the absence of Mg^{2+}.

Mg^{2+} Titration Experiments. To explore the minimum Mg^{2+} concentration necessary for tertiary folding of unmodified yeast tRNA^{Phe}, we investigated tertiary structure formation as a function of [Mg^{2+}] under equilibrium conditions. UV cross-linking was used to monitor the structure of the hinge region in 100 mM Na^+ buffers containing 0−10 mM Mg^{2+} (because the Pb^{2+} cleavage assay is dependent on [Mg^{2+}], it cannot be used for these studies; *21*). At 20 °C, the rate of UV cross-link formation increased until [Mg^{2+}] = 3 mM, after which the rate remained constant (Figure 4). Thus, in buffers containing <3 mM Mg^{2+}, it appears that tertiary structure at the hinge region is not completely formed. Our findings are in general agreement with those of Friederich and Hagerman (*39*), who report that the largest changes in the interstem angle of unmodified yeast tRNA^{Phe} upon going from secondary to tertiary structure (as monitored by transient electric birefringence at 4 °C) occur in 200 μM Mg^{2+}, with further reduction of the angle occurring up to 4 mM Mg^{2+}.

Changes in the CD spectrum of unmodified yeast tRNA^{Phe} were also measured as a function of [Mg^{2+}]. In both the presence and absence of Mg^{2+}, the principal maximum and

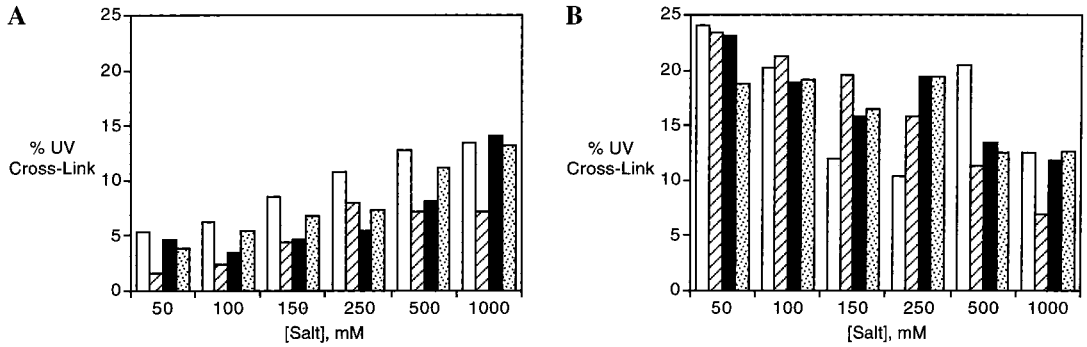

FIGURE 3: Ultraviolet cross-linking of [5′-^{32}P] unmodified yeast tRNA^{Phe} for 15 min at 20 °C in (A) 10 mM NaCac, 90 mM NaCl, pH 6.8, or (B) 10 mM NaCac, 90 mM NaCl, 5 mM $MgCl_2$, pH 6.8, with varying amounts of LiCl, NaCl, KCl, and NH_4Cl. Dotted bar, NH_4Cl; open bar, LiCl; hatched bar, NaCl; black bar, KCl. Standard deviation in these measurements is ca. ±3%. In the presence of Mg^{2+}, the amount of UV cross-link formation decreases as the monovalent salt concentration increases, suggesting either that proper tertiary structure is not forming or that the population of correctly folded tRNAs is decreasing. Similar effects have previously been observed for yeast tRNA^{Val} (*42*) and for an RNA pseudoknot (*43*) and probably arise from a competition between Mg^{2+} and Na^+ for binding sites on the RNA (*43*).

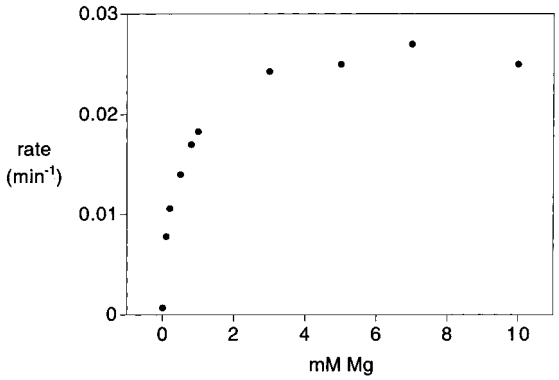

FIGURE 4: UV cross-link formation as a function of [Mg^{2+}]. Experiments performed with [5′-^{32}P] unmodified yeast tRNA^{Phe} in 10 mM NaCac, 90 mM NaCl, pH 6.8, at 25 °C.

minimum occur at 261 and 207 nm, respectively (Figure 5 top). Titration of Mg^{2+} to 1 mM produces a large change in the molar ellipticity at 207 nm (40%) while further addition of Mg^{2+} (to 20 mM) does not alter the CD spectrum. The small increase at 260 nm observed with rising [Mg^{2+}] suggests that Mg^{2+} does not alter base stacking within the tRNA to an appreciable extent, while the large increase at 207 nm may be due to subtle changes in base stacking involving the loops of the tRNA, and possible alterations in the tilt of bases in helical regions (*44*). Similar spectroscopic changes were observed for the transition from secondary to tertiary structure in native yeast tRNA^{Phe} induced by addition of Mg^{2+} to a 32 mM Na^+ buffer at 40 °C (Figure 5, middle; *34*, *35*). By contrast, addition of Mg^{2+} to yeast tRNA^{Phe} under conditions where tertiary structure is stable in the absence of Mg^{2+} (32 mM Na^+, 15 °C) produces no significant spectral changes (Figure 5, bottom; *34*, *35*). These observations indicate that the main conformational transition from secondary to tertiary structure occurs at [Mg^{2+}] = 1 mM, and suggest that the increase in UV cross-linking rate observed from 1 to 3 mM Mg^{2+} may be due to the hinge region becoming more compact and the residues involved in the UV cross-link becoming more proximal.

To address the nature of Mg^{2+} binding to unmodified yeast tRNA^{Phe}, UV thermal denaturation experiments were conducted as a function of [Mg^{2+}] in a 100 mM Na^+ buffer. A single monophasic transition is observed for [Mg^{2+}] from 500 μM to 15 mM at 260 nm. From these data, plots of T_m vs log [Mg^{2+}] were constructed for comparison with yeast tRNA^{Phe}. The slope of the plot for unmodified yeast tRNA^{Phe} in 100 mM Na^+ is the same as the slope for yeast tRNA^{Phe} determined under the same conditions (Figure 6). This similarity suggests that both the binding modes and the number of Mg^{2+} ions bound to unmodified yeast tRNA^{Phe} are probably similar to the native tRNA (*45*−*50*).

Secondary Structure Mapping of Unmodified Yeast tRNA^{Phe}. Most of the base modifications in native yeast tRNA^{Phe} are located in the loop regions while Watson−Crick pairing with the canonical bases is maintained in the helical stems. Therefore, the cloverleaf secondary structures of both native and unmodified yeast tRNA^{Phe} should have similar stability. Deconvolution of the molar heat capacity curve obtained from differential scanning microcalorimetry experiments suggests that in the absence of Mg^{2+}, there are four structural transitions in the thermal denaturation pathway of unmodified yeast tRNA^{Phe} (data not shown). The deconvolutions of both calorimetric (*35*) and UV thermal denaturation curves (*34*) for native yeast tRNA^{Phe} show that the latter four of the five observed transitions are associated with secondary structure melting and have T_m and ΔH values similar to those observed for unmodified yeast tRNA^{Phe}. These results suggest the secondary structures of unmodified yeast tRNA^{Phe} and native yeast tRNA^{Phe} are similar and that denaturation of the cloverleaf may proceed in a similar manner in both tRNAs.

To determine if the canonical cloverleaf model accurately predicts the secondary structure of unmodified yeast tRNA^{Phe}, we probed the structure of unmodified yeast tRNA^{Phe} in 100 mM Na^+ in the absence of Mg^{2+}. The primary cleavages observed with the single-strand-specific enzymes nuclease S1, Rn nuclease I (*51*, *52*), and RNase T2 at 25 °C occur in the anticodon loop (Figure 7). As a group, these enzymes also recognize all positions within the D-loop, with RNase T2 cleaving primarily at residues U16 and U17, while nuclease S1 and Rn nuclease I cleave at G15, U16, U17, G18, G19, and G20. Rn nuclease I also recognizes most positions within the T-loop (U55, C56, G57, and A58). RNase V1, a double-strand-specific ribonuclease, cuts at positions within each helical region with nearly equal intensity. Cleavage occurs at positions on both the 5′ and 3′ sides of the D-stem, at C28, U41, and G42 within the anticodon stem, and at residues U50, G51, U52, C63, A64, and G65 in the T-stem. Every position in the acceptor stem

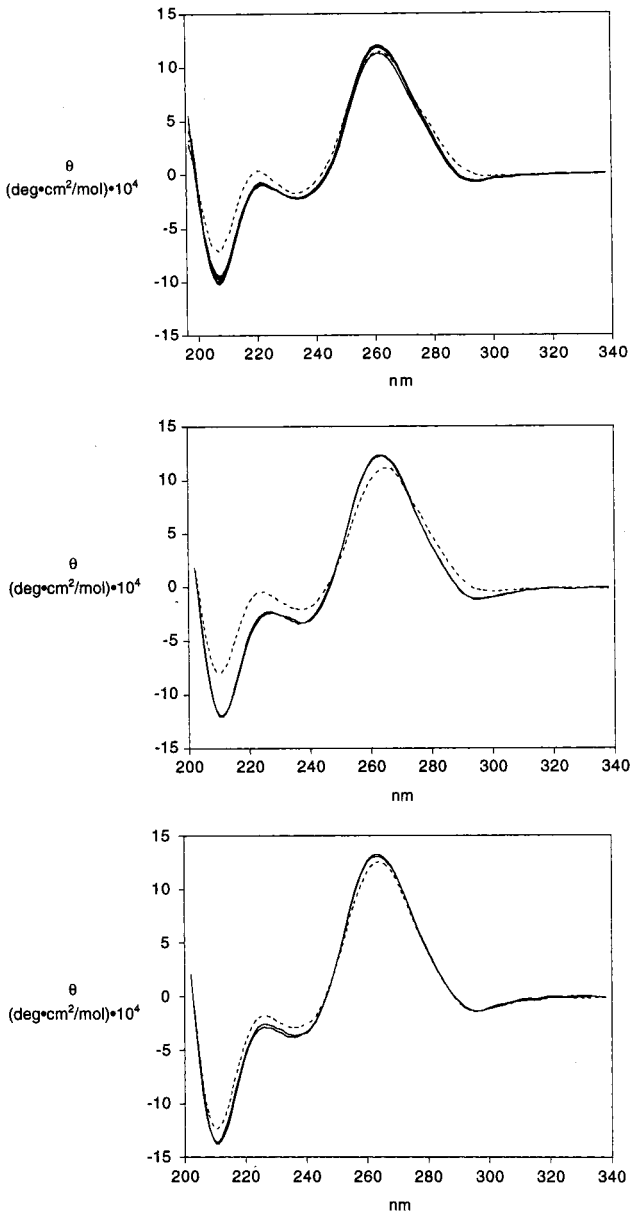

FIGURE 5: CD spectra measured in 10 mM NaCac, 90 mM NaCl, pH 6.8, as a function of $[Mg^{2+}]$ at 25 °C. (Top) Unmodified yeast $tRNA^{Phe}$. The data at 0 mM Mg^{2+} are denoted with a dashed line (- - -). The data at $[Mg^{2+}] = 1$, 2, 5, 10, and 20 mM are identical and are shown with the solid line (—). CD spectra of native yeast $tRNA^{Phe}$ measured in 10 mM NaCac, 22 mM NaCl, pH 6.8, as a function of Mg^{2+}. The middle and bottom panels show data measured at 40 and 15 °C, respectively, where the data at 0 mM Mg^{2+} are denoted with a dashed line (- - -). The spectra measured with $[Mg^{2+}] = 0.5$ and 1 mM are identical and are shown with the solid line (—). DMS footprinting in these buffers is consistent with the conclusion that at 15 °C yeast $tRNA^{Phe}$ adopts tertiary structure in both the presence and absence of Mg^{2+}, while at 37 °C Mg^{2+} is necessary for tertiary structure formation (data not shown).

is also cleaved by RNase V1. Finally, cleavage by RNase V1 is not observed at any residues located in single-stranded regions of the cloverleaf model.

Several residues predicted by the cloverleaf model to be base-paired and located either at a stem−loop junction or at the four-way junction are recognized by the single-stranded enzymes: G10 and C13 in the D-stem, G43 in the anticodon stem, C61 and G53 in the T-stem. This finding suggests that these base pairs either are frayed or are not formed,

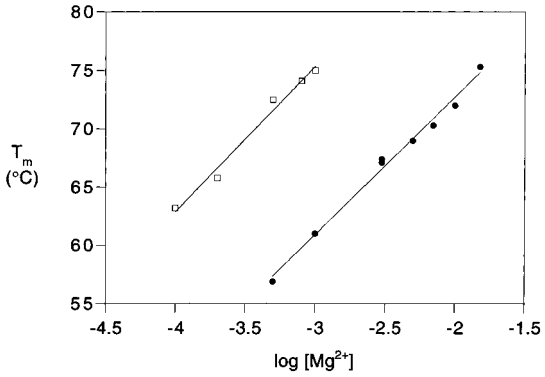

FIGURE 6: Plot of T_m vs log $[Mg^{2+}]$ obtained from thermal denaturation experiments monitored at 260 nm. Unmodified yeast $tRNA^{Phe}$ (●); yeast $tRNA^{Phe}$ (□). The slope for unmodified yeast $tRNA^{Phe}$ is 11.8 ± 0.5, and the slope for yeast $tRNA^{Phe}$ is 12.5 ± 0.9.

which is not unexpected for base pairs at loops or junctions (*53*). Cleavage with nuclease S1 is also observed at G42, the penultimate base pair at the 3′-end of the anticodon stem. However, G42 is also cleaved by RNase V1, which suggests that in this region the phosphate backbone adopts a conformation that is recognized by both single- and double-stranded enzymes. Additionally, residue A23 within the D-stem is recognized by RNase T2. In this case, however, cleavage also occurs in the presence of Mg^{2+}, conditions under which the U12−A23 base pair is formed (*23*). This observation indicates either that this region is weakly base-paired in both the secondary and tertiary structures (*54*) or that the backbone conformation is not standard A-form in this region. The crystal structure of yeast $tRNA^{Phe}$ shows that the D-stem differs from standard A-form geometry (more than any of the other helical regions; *55*) which supports the latter interpretation.

In addition to the enzymatic probes, we also mapped the cloverleaf secondary structure of unmodified $tRNA^{Phe}$ by strand scission following treatment with DEPC, and by primer extension after reaction with either DMS or CMCT. At 25 °C, which is below the temperature where thermal denaturation occurs, DEPC predominantly modifies the anticodon loop of unmodified yeast $tRNA^{Phe}$ at residues A35, A36, and A38, and also at residues A9, A14, A44, and A58, which are predicted to be single-stranded (Figure 2). Modification with DMS also occurs at single-stranded residues, including C32 in the anticodon loop as well as every adenosine residue modified by DEPC. CMCT modifies residues in each of the single-stranded regions of the tRNA: U8 which is at the juncture of the acceptor and the D-stems; G15, U16, and G20 in the D-loop; U33, G34, and G37 in the anticodon loop; G45, G46, and U47 in the variable loop; and U54, U55, G57, and U59 in the T-loop. Importantly, residues predicted to be within helical regions by the canonical cloverleaf model are protected from modification by DEPC, DMS, and CMCT, with the exception of U39 which is involved in a base pair at the anticodon stem−loop junction. Furthermore, the residues located in helical regions that were cleaved by the single-stranded enzymes are not modified by these reagents (vide supra). These data further support our conclusion that both the anticodon stem and the D-stem possess atypical backbone conformations that allow

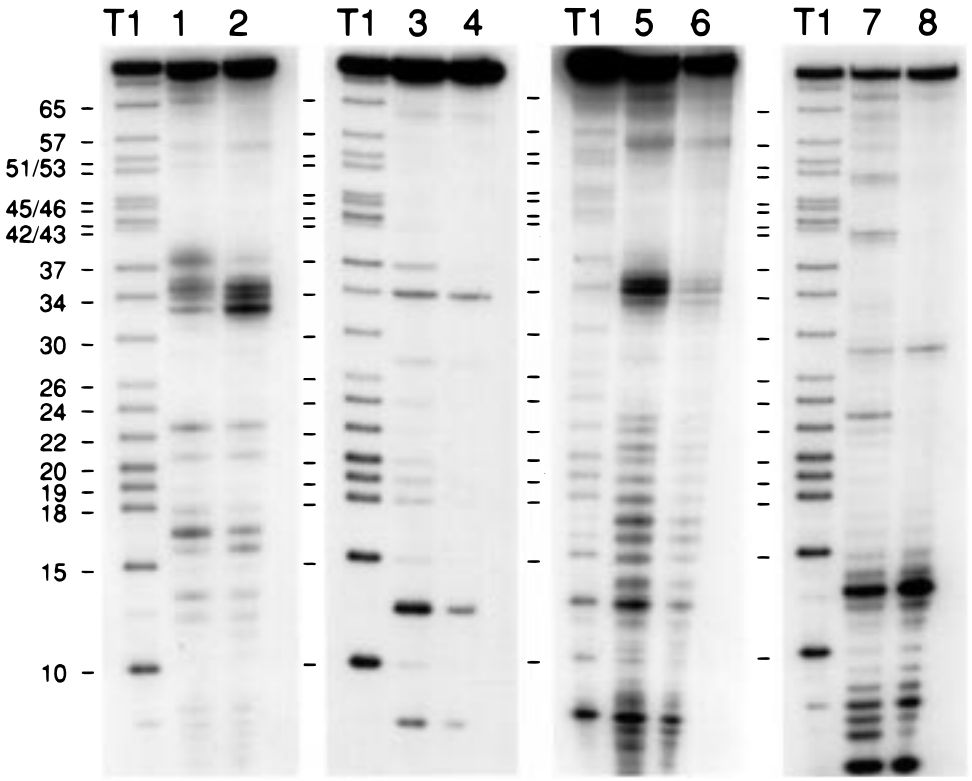

FIGURE 7: Enzymatic cleavage of [5′-^{32}P] unmodified yeast tRNA^{Phe} in either 10 mM NaCac, 90 mM NaCl, pH 6.8, or 10 mM NaCac, 90 mM NaCl, 5 mM $MgCl_2$, pH 6.8, at 25 °C. T1, denaturing RNase T1 ladder; lane 1, RNase T2; lane 2, RNase T2, 5 mM Mg^{2+}; lane 3, nuclease S1; lane 4, nuclease S1, 5 mM Mg^{2+}; lane 5, Rn nuclease I; lane 6, Rn nuclease I, 5 mM Mg^{2+}; lane 7, RNase V1; lane 8, RNase V1, 5 mM Mg^{2+}. Similar results are obtained at 35 °C. Assignments have also been confirmed using [3′-^{32}P]tRNA (data not shown).

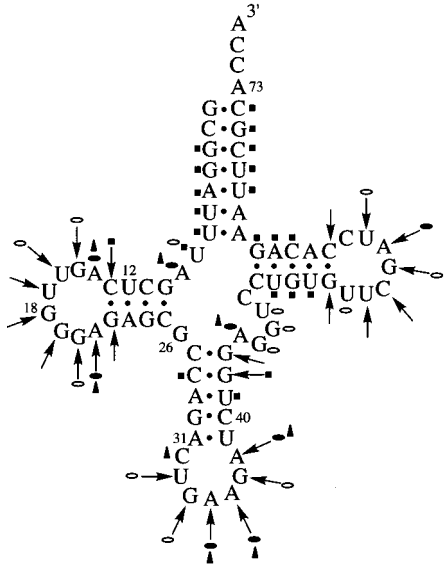

FIGURE 8: Cloverleaf secondary structure of unmodified yeast tRNA^{Phe} summarizing results of chemical and enzymatic footprinting experiments in 10 mM NaCac, 90 mM NaCl, pH 6.8. Bold arrow, single-strand enzymes; solid square, RNase V1; solid oval, DEPC; solid triangle, DMS; open oval, CMCT.

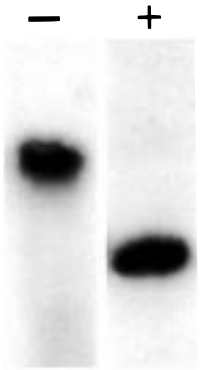

FIGURE 9: Native gel electrophoresis of 5′-^{32}P unmodified yeast tRNA^{Phe} in 10 mM NaCac, 90 mM NaCl, pH 6.8, in both the presence (+) and the absence (−) of 5 mM Mg^{2+}.

recognition by single-strand-specific enzymes. Taken together, the results of both the chemical and enzymatic footprinting indicate that the canonical cloverleaf secondary structure of unmodified yeast tRNA^{Phe} forms in 100 mM Na^+ in the absence of Mg^{2+} (Figure 8).

Approximate Phase Diagrams. Our data indicate that unmodified yeast tRNA^{Phe} exists in either the cloverleaf secondary structure or the tertiary structure depending on the presence of Mg^{2+}. Below the T_m of the cloverleaf, unmodified yeast tRNA^{Phe} migrates on native gels as a single band in both the presence and the absence of Mg^{2+}, with the tertiary folded species migrating faster than the cloverleaf (Figure 9). These results suggest that unmodified yeast tRNA^{Phe} exists in a Mg^{2+}-dependent equilibrium between tertiary folded and cloverleaf structures, and this interconversion is rapid on the electrophoresis time scale (see *56* for a similar example). Based on these data and those presented below, we have constructed approximate phase diagrams illustrating the conformational states of unmodified yeast tRNA^{Phe} in either the presence or the absence of Mg^{2+} (Figure 10A). These diagrams are of lower resolution than the more conventional conformation-phase diagrams constructed from thermal denaturation experiments. Neverthe-

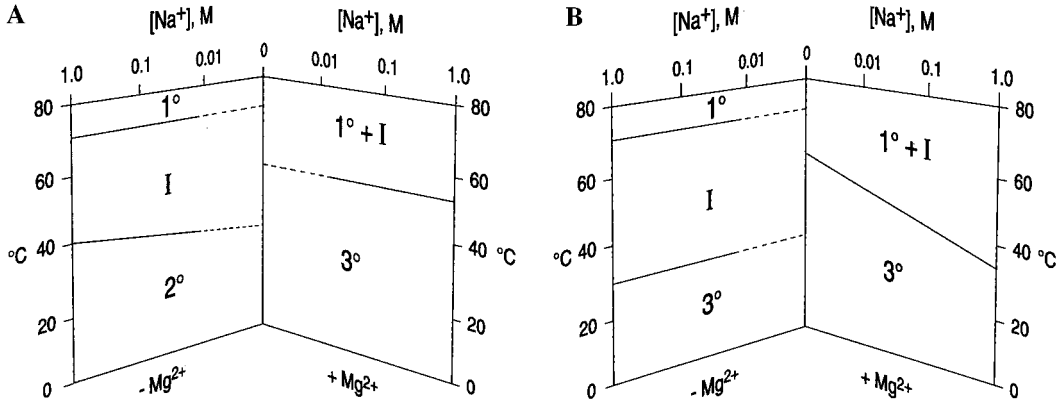

FIGURE 10: Appoximate phase diagrams for (A) unmodified yeast tRNA^{Phe} and (B) yeast tRNA^{Phe}; 1°, random coil; 2°, cloverleaf secondary structure; 3°, tertiary structure; I, intermediate denatured states. Dashed lines indicate that no data are available at these [Na^+]. The yeast tRNA^{Phe} diagram was constructed from melting data previously obtained in similar buffers (*57*−*68*).

less, they are useful for summarizing the data presented here.

Although the Mg^{2+} titration experiments suggest that elements of tertiary structure are formed in less than 5 mM Mg^{2+}, the highest resolution structural evidence that unmodified yeast tRNA^{Phe} adopts native tertiary structure was obtained through ^{1}H NMR measurements conducted in 5 mM Mg^{2+} buffer (*23*). Therefore, the phase diagram in the presence of Mg^{2+} was constructed from data obtained at 5 mM Mg^{2+}. The solid line separating secondary structure from intermediate states in the absence of Mg^{2+} is estimated from both calorimetry and the results of structure probing experiments described above conducted at 25 and 35 °C. The solid line at 70 °C in the absence of Mg^{2+} is estimated from the upper base line of thermal denaturation curves obtained as a function of [Na^+] (15 mM to 1 M). The solid line separating tertiary structure from random coil and intermediate states in 5 mM Mg^{2+} is determined from T_m values of thermal denaturation curves obtained in 5 mM Mg^{2+} as a function of [Na^+]. The differences we have observed in the conformational properties of unmodified and native yeast tRNA^{Phe} are highlighted by comparison with the approximate phase diagram for yeast tRNA^{Phe} (Figure 10B).

Unfolding Kinetics of Unmodified Yeast tRNA^{Phe}. Very little information exists about the rate-determining transition states (RDS) for RNA tertiary structure folding. A solution to the RNA folding problem clearly must address the structural and energetic role of tertiary interactions in both the ground state and the RDS of tertiary folding in much greater detail. We have previously demonstrated that the rate and activation parameters of tertiary structure unfolding can be measured for yeast tRNA^{Phe} using a "Mg^{2+}-jump" experiment (*69*). This method entails mixing an RNA solution containing Mg^{2+} with excess EDTA under conditions of temperature and ionic strength where tertiary structure unfolds to the cloverleaf after chelation of Mg^{2+}. By using a stopped-flow instrument to perform the mixing, low millisecond resolution can be achieved and the unfolding transition can be observed by UV absorbance.

Since the tertiary structure of unmodified yeast tRNA^{Phe} exists in a Mg^{2+}-dependent equilibrium, Mg^{2+}-jump kinetics can also be used to measure the rate of tertiary structure unfolding. Based on the studies presented above, we propose

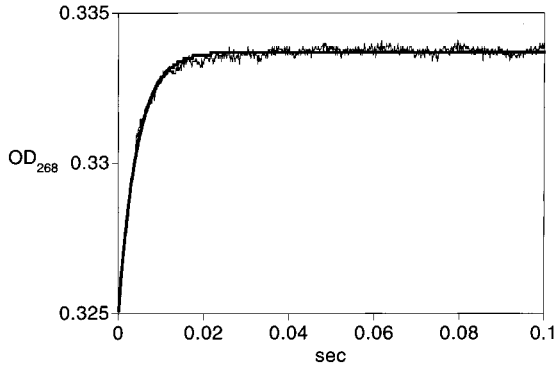

FIGURE 11: Average of nine kinetic traces obtained at 23.0 °C for the rapid mixing of unmodified yeast tRNA^{Phe} with 30 mM EDTA. The solid bold line is the first-order exponential fit to the observed rate data. In general, residuals to the fits range from 9×10^{-4} to 3×10^{-3}.

that unfolding of unmodified yeast tRNA^{Phe} can be given by eq 1 (*70*):

$$\text{tRNA(3°)}\cdot Mg^{2+} \underset{k_{-1}}{\overset{k_1}{\rightleftharpoons}} \text{tRNA(2°)}\cdot Mg^{2+} + Mg^{2+} \xrightarrow[k_2]{\text{EDTA}} \text{tRNA(2°)} \quad (1)$$

When a solution of folded unmodified yeast tRNA^{Phe} in a pH 6.8 buffer containing 100 mM Na^+ and 5 mM Mg^{2+} is mixed with a 30 mM EDTA buffer, an increase in hyperchromicity is observed (Figure 11). The rates obtained from measurements conducted as a function of temperature range from 233 s^{-1} at 20.2 °C to 955 s^{-1} at 31.7 °C. In all cases, monophasic kinetics are observed with an absorbance change of about 3%, which agrees with that observed in melting curves obtained in both the presence and absence of Mg^{2+}. A hyperchromicity difference of this magnitude is characteristic of tertiary folding transitions in tRNAs (*39*, *45*, *60*, *71*, *77*). In two important controls, we find that replacing EDTA with NaOAc produces no hyperchromic change, and at [EDTA] < [Mg^{2+}] no hyperchromic shift is observed. Taken together, these results provide further evidence that the hyperchromic change is due to tertiary unfolding. While some unfolding may occur when [EDTA] < [Mg^{2+}], under these conditions the associated absorbance change is too small to observe.

Mg^{2+}-jump experiments will monitor tertiary unfolding of unmodified yeast tRNA^{Phe} provided that the off-rate of

Mg^{2+} from the tRNA in the presence of chelator is sufficiently fast so that the rate-determining step is unfolding, rather than the dissociation of Mg^{2+}. In other words, it is necessary that k_2[EDTA] $\gg k_{-1}$, so that $k_{obs} = k_1$. Under these conditions, k_{obs} should be independent of [EDTA]. To determine when this condition is satisfied, Mg^{2+}-jump experiments were conducted as a function of [EDTA]. At EDTA concentrations at least 2-fold higher than the Mg^{2+} concentration, the rates of the observed transition are constant, which indicates that the observed transition reflects solely tertiary unfolding, uncomplicated by Mg^{2+} dissociation. Moreover, using chelators with slower on-rates for Mg^{2+} relative to EDTA (e.g., CDTA; *73*) results in complicated multiphasic kinetics. By contrast, chelating reagents that are thought to bind Mg^{2+} with similar on-rates as EDTA (i.e., 1,2-diaminopropane-*N*,*N*,*N*′,*N*′-tetraacetic acid) afford comparable rate data to those obtained using EDTA (data not shown).

Eyring plots were constructed using rate data for each [EDTA] $\geq$ 10 mM, and afford an activation free energy ($\Delta G^{\ddagger}$) for tertiary structure unfolding of 14 $\pm$ 0.7 kcal/mol. The linearity of the Eyring plots suggests that there is not a large difference in heat capacity between the tertiary folded state and the cloverleaf. Thus, it is likely that the degree of base stacking in both conformations is similar, which is consistent with the small hyperchromicity difference measured for tertiary unfolding (*39*). The corresponding $\Delta G^{\ddagger}$ for unfolding of yeast $tRNA^{Phe}$ calculated from data presented in Maglott and Glick (*69*) is 15.5 kcal/mol. This increase relative to unmodified yeast $tRNA^{Phe}$ results primarily from a more favorable activation entropy, 52 $\pm$ 2 cal/(mol·K) and 27 $\pm$ 4 cal/(mol·K) for unmodified and native yeast $tRNA^{Phe}$, respectively. This difference in entropy undoubtedly has several origins, including differential solvation, differential counterion binding/release, and differences in configurational entropy. These results suggest that the posttranscriptional modifications create a more ordered transition state of unfolding and are consistent with the observation that yeast $tRNA^{Phe}$ is more stable than unmodified yeast $tRNA^{Phe}$ at equilibrium (*6*).

DISCUSSION

There is a remarkable similarity of tertiary structure among tRNAs that is due in part to the high level of conservation of residues within the single-stranded loops (*74*). Although tRNAs from different organisms share conserved residues and global tertiary structure, the number, location, and identity of posttranscriptional modifications vary between sequences (*75*). Since these modified residues play a role in stabilizing tertiary structure (*3*−*6*, *23*), the conformational transitions and the stability of various states may not be the same for all tRNAs. Significant differences also can exist between native tRNAs and their unmodified counterparts. Understanding these differences is especially important if unmodified tRNAs are used as models for the native systems.

Tertiary folding of 5 unmodified tRNAs has been studied using direct structural probing (*3*, *5*, *18*−*24*), and the folding of at least 10 others has been examined in functional assays. All but one of these sequences adopts the canonical L-shaped tertiary structure in the presence of Mg^{2+} (*3*). Tertiary folding of four unmodified tRNAs has been examined in depth, and for each of these four tRNAs, a higher [Mg^{2+}] relative to the corresponding native tRNA is required to produce tertiary structure (*4*−*6*, *22*) which indicates that the posttranscriptionally modified bases can affect the stability of secondary and tertiary structure. Our studies of unmodified yeast $tRNA^{Phe}$ show that in contrast to the native sequence, formation of tertiary structure has an absolute requirement for Mg^{2+}: removal of the posttranscriptional modifications alters the intrinsic stability of tertiary structure significantly. However, it is not yet known if this strict need for Mg^{2+} is applicable to other unmodified tRNA constructs.

Using both thermodynamic and kinetic measurements, Crothers and co-workers investigated the conformation of four *Escherichia coli* tRNAs (Phe, fMet, Tyr, and Val) as a function of temperature and [Na^+] (*33*). Conformation-phase diagrams constructed from these measurements consist of four regions: native, cloverleaf or close variants, coil, and extended forms (*33*). With the exception of the true cloverleaf secondary structure, direct evidence that bacterial tRNAs can assume all conformational states defined by Crothers has been obtained (*76*, *77*). The low [Na^+] and low-temperature region in which *Escherichia coli* tRNAs adopt extended structure is defined by breaks in plots of T_m vs log [Na^+]. Similar plots for both unmodified and native yeast $tRNA^{Phe}$ have continuous linear slopes throughout the range of [Na^+], indicating that a distinct low-[Na^+] and low-temperature form of these tRNAs is not populated. In fact, our footprinting data demonstrate that unmodified yeast $tRNA^{Phe}$ adopts the canonical cloverleaf secondary structure in the low-[Na^+] and low-temperature region of Crothers' phase diagrams. Hence, our data argue that a single phase diagram cannot describe all "tRNA folding".

Some posttranscriptional modifications present in tRNAs are unique to either eukaryotes or prokaryotes, with eukaryotic tRNAs typically containing more modified nucleosides than prokaryotic sequences (*75*). It is clear that different posttranscriptional modifications exert varying influence on the structure and stability of tRNAs (e.g., bacterial tRNAs form extended secondary structures under conditions where native yeast $tRNA^{Phe}$ adopts tertiary structure; *33*−*35*). Although the influence of specific posttranscriptional modifications is known for only a few modified nucleosides, a single modified residue can have a dramatic impact on structure and stability. For instance, chemical excision of wybutosine in the anticodon loop in yeast $tRNA^{Phe}$ not only changes the structure of the anticodon loop (*78*) but also alters the accessibility of the D- and T-loop regions to oligonucleotide and chemical probing (*79*, *80*) which suggests that wybutosine influences tertiary structure in regions of the tRNA distal to the site of modification. Other posttranscriptional modifications increase the thermal stability of a tRNA (*24*, *81*−*83*). For example, the presence of the highly conserved ribothymidine at position 54 of the T-loop in prokaryotic tRNAs increases the T_m of *Escherichia coli* $tRNA^{f,Met}$ by 6 °C compared to a mutant containing U54 (*83*). However, it is not known whether all of the posttranscriptionally modified nucleosides are equally necessary or if some have greater effects than others on tertiary and secondary structure formation. To fully understand tRNA folding, a comprehensive analysis of the structural properties of tRNAs as a function of both primary sequence and posttranscriptional modifications is necessary.

Since posttranscriptional modifications are generally not found in other cellular RNAs, unmodified tRNAs appear well-suited model systems for examining general aspects of RNA folding. For example, it has been shown recently that the tertiary structure of the P4−P6 domain of the *Tetrahymena thermophila* group I intron exists in a Mg^{2+}-dependent equilibrium between tertiary and secondary structure (*56*). Both the tertiary structure of the P4−P6 domain and the manner in which it interacts with Mg^{2+} apparently are different from tRNAs. Yet, our results suggest that unmodified yeast $tRNA^{Phe}$ is also in a Mg^{2+}-dependent equilibrium between tertiary and secondary structure. Furthermore, it appears that a similar equilibrium is not present for yeast $tRNA^{Phe}$, even though our thermal denaturation data indicate the mode of binding of Mg^{2+} to unmodified yeast $tRNA^{Phe}$ is similar to native yeast $tRNA^{Phe}$. It is possible, therefore, that this conformational equilibrium is not dependent on the mode of Mg^{2+} binding but rather that divalent ions compensate for the lack of posttranscriptional modifications which themselves act to stabilize tertiary structure (*23*).

CONCLUSIONS

Through chemical probing experiments, we have provided direct structural evidence to support the hypothesis that native yeast $tRNA^{Phe}$ adopts tertiary structure in the absence of Mg^{2+}. Under identical conditions, unmodified yeast $tRNA^{Phe}$ does not undergo tertiary folding and only the cloverleaf secondary structure forms. This observation clearly demonstrates the profound effect that the posttranscriptionally modified bases can have on the intrinsic stability of tRNA tertiary structure, and begins to define the limitations of synthetic tRNAs as models for native tRNAs. Since there are pronounced sequence-dependent differences in the conformational states of tRNAs, broad conclusions regarding "tRNA folding" as a whole must be viewed cautiously, particularly in cases where structural changes occur, such as during protein synthesis.

ACKNOWLEDGMENT

We thank O. C. Uhlenbeck for plasmid p67YF0/DH5αF′, F. W. Studier for plasmid pAR1219/BL21, G. Garcia for advice on in vitro transcription of unmodified yeast $tRNA^{Phe}$, and D. Ballou for assistance with interpretation of the kinetic data.

REFERENCES

1. Bjork, G. R. (1995) in *tRNA Structure, Biosynthesis, and Function* (Söll, D., and RajBhandary, U. L., Eds.) pp 165−205, ASM Press, Washington, D.C.
2. Yokoyama, S., and Nishimura, S. (1995) in *tRNA Structure, Biosynthesis, and Function* (Söll, D., and RajBhandary, U. L., Eds.) pp 207−223, ASM Press, Washington, D.C.
3. Helm, M., Brulé, H., Degoul, F., Cepanec, C., Leroux, J.-P., Giegé, R., and Florentz, C. (1998) *Nucleic Acids Res. 26*, 1636−1643.
4. Serebrov, V. Yu., Vasilenko, K. S., Kholod, N. S., and Kiselev, L. L. (1997) *Mol. Biol. 31*, 762−767.
5. Kintanar, A., Yue, D., and Horowitz, J. (1994) *Biochimie 76*, 1192−1204.
6. Sampson, J. R., and Uhlenbeck, O. C. (1988) *Proc. Natl. Acad. Sci. U.S.A. 85*, 1033−1037.
7. Goodwin, J. T., Stanick, W. A., and Glick, G. D. (1994) *J. Org. Chem. 59*, 7941−7942.
8. Moor, N. A., Ankilova, V. N., and Lavrik, O. I. (1995) *Eur. J. Biochem. 234*, 897−902.
9. Avis, J. M., Day, A. G., Garcia, G. A., and Fersht, A. R. (1993) *Biochemistry 32*, 5312−5320.
10. Peterson, E. T., and Uhlenbeck, O. C. (1992) *Biochemistry 31*, 10380−10389.
11. Beresten, S., Jahn, M., and Söll, D. (1992) *Nucleic Acids Res. 20*, 1523−1530.
12. Jahn, M., Rogers, M. J., and Söll, D. (1991) *Nature 352*, 258−260.
13. Perret, V., Garcia, A., Grosjean, H., Ebel, J. P., Florentz, C., and Giegé, R. (1990) *Nature 344*, 787−789.
14. Schulman, L. H., and Pelka, H. (1990) *Nucleic Acids Res. 18*, 285−289.
15. Samuelsson, T., Boren, T., Johansen, T.-I., and Lustig, F. (1988) *J. Biol. Chem. 263*, 13692−13699.
16. Harrington, K. M., Nazarenko, I. A., Dix, D. B., Thompson, R. C., and Uhlenbeck, O. C. (1993) *Biochemistry 32*, 7617−7622.
17. Curnow, A. W., Kung, F.-L., Koch, K. A., and Garcia, G. A. (1993) *Biochemistry 32*, 5239−5246.
18. Han, H., and Dervan, P. B. (1994) *Proc. Natl. Acad. Sci. U.S.A. 91*, 4955−4959.
19. Derrick, W. B., and Horowitz, J. (1993) *Nucleic Acids Res. 21*, 4948−4953.
20. Behlen, L. S., Sampson, J. R., and Uhlenbeck, O. C. (1992) *Nucleic Acids Res. 20*, 4055−4059.
21. Behlen, L. S., Sampson, J. R., DiRenzo, A. B., and Uhlenbeck, O. C. (1990) *Biochemistry 29*, 2515−2523.
22. Perret, V., Garcia, A., Puglisi, J., Grosjean, H., Ebel, J. P., Florentz, C., and Giegé, R. (1990) *Biochimie 72*, 735−744.
23. Hall, K. B., Sampson, J. R., Uhlenbeck, O. C., and Redfield, A. G. (1989) *Biochemistry 28*, 5794−5801.
24. Arnez, J. G., and Steitz, T. A. (1994) *Biochemistry 33*, 7560−7567.
25. Sampson, J. R. (1989) Ph.D. Thesis, University of Colorado, Boulder, CO.
26. Goodwin, J. T., Osborne, S. E., Scholle, E. J., and Glick, G. D. (1996) *J. Am. Chem. Soc. 118*, 5207−5215.
27. Scaringe, S. A., Francklyn, C., and Usman, N. (1990) *Nucleic Acids Res. 18*, 5433−5441.
28. Przykorska, A., and Szarkowski, J. W. (1980) *Eur. J. Biochem. 108*, 285−293.
29. England, T. E., and Uhlenbeck, O. C. (1978) *Nature 275*, 560−561.
30. Peattie, D. A., and Gilbert W. (1980) *Proc. Natl. Acad. Sci. U.S.A. 77*, 4679−4682.
31. Zueva, V. S., Mankin, A. S., Bogdanov, A. A., and Baratova, L. A. (1985) *Eur. J. Biochem. 146*, 679−687.
32. Banerjee, A. R., Jaeger, J. A., and Turner, D. H. (1993) *Biochemistry 32*, 153−163.
33. Cole, P. E., Yang, S. K., and Crothers, D. M. (1972) *Biochemistry 11*, 4358−4368.
34. Coutts, S. M., Riesner, D., Römer, R., Rabl, C. R., and Maass, G. (1975) *Biophys. Chem. 3*, 275−289.
35. Privalov, P. L., and Filimonov, V. V. (1978) *J. Mol. Biol. 122*, 447−464.
36. Riesner, D., Maass, G., Thiebe, R., Philippsen, P., and Zachau, H. G. (1973) *Eur. J. Biochem. 36*, 76−88.
37. Urbanke, C., Römer, R., and Maass, G. (1973) *Eur. J. Biochem. 33*, 511−516.
38. Hinz, H.-J., Filimonov, V. V., and Privalov, P. L. (1977) *Eur. J. Biochem. 72*, 79−86.
39. Friederich, M. W., and Hagerman, P. J. (1997) *Biochemistry 36*, 6090−6099.
40. Ehresmann, C., Baudin, F., Mougel, M., Romby, P., Ebel, J.-P., and Ehresmann, B. (1987) *Nucleic Acids Res. 15*, 9109−9128.
41. Romby, P., Moras, D., Dumas, P., Ebel, J. P., and Giegé, R. (1987) *J. Mol. Biol. 195*, 193−204.
42. Privalov, P. L., Filimonov, V. V., Venkstern, T. V., and Bayev, A. A. (1975) *J. Mol. Biol. 97*, 279−288.
43. Gluick, T. C., Gerstner, R. B., and Draper, D. E. (1997) *J. Mol. Biol. 270*, 451−463.

44. Willick, G. E., and Kay, C. M. (1971) *Biochemistry 10*, 2216−2222.
45. Guéron, M., and Leroy, J. L. (1982) *Biophys. J. 38*, 231−236.
46. Leroy, J.-L., Guéron, M., Thomas, G., and Favre, A. (1977) *Eur. J. Biochem. 74*, 567−574.
47. Leroy, J.-L., and Guéron, M. (1977) *Biopolymers 16*, 2429−2446.
48. Walters, J. A. L. I., Geerdes, H. A. M., and Hilbers, C. W. (1977) *Biophys. Chem. 7*, 147−151.
49. Plum, G. E., and Breslauer, K. J. (1995) *J. Mol. Biol. 248*, 679−695.
50. Record, M. T., Jr., Woodbury, C. P., and Lohman, T. M. (1976) *Biopolymers 15*, 893−915.
51. Przykorska, A., El Adlouni, C., Keith, G., Szarkowski, J. W., and Dirheimer, G. (1992) *Nucleic Acids Res. 20*, 659−663.
52. Przykorska, A. (1995) *Biochimie 77*, 109−112.
53. Kan, L. S., Borer, P. N., and Ts'o, P. O. P (1975) *Biochemistry 14*, 4864−4869.
54. Lockard, R. E., and Kumar, A. (1981) *Nucleic Acids Res. 9*, 5125−5140.
55. Holbrook, S. R., Sussman, J. L., Warrant, R. W., and Kim, S.-H. (1978) *J. Mol. Biol. 123*, 631−660.
56. Szewczak, A., and Cech, T. R. (1997) *RNA 3*, 838−849.
57. Heerschap, A., Mellema, J.-R., Janssen, H. G. J. M., Walters, J. A. L. I., Haasnoot, C. A. G., and Hilbers, C. W. (1985) *Eur. J. Biochem. 149*, 649−655.
58. Hilbers, C. W., Heerschap, A., Haasnoot, C. A. G., and Walters, J. A. L. I. (1983) *J. Biomol. Struct. Dyn. 1*, 183−207.
59. Li, Z. Q., Giegé, R., Jacrot, B., Oberthür, R., Thierry, J.-C., and Zaccaï, G. (1983) *Biochemistry 22*, 4380−4388.
60. Aultman, K. S., and Chang, S. H. (1982) *Eur. J. Biochem. 124*, 471−476.
61. Johnston, P. D., and Redfield, A. G. (1981) *Biochemistry 20*, 1147−1156.
62. Johnston, P. D., and Redfield, A. G. (1981) *Biochemistry 20*, 3996−4006.
63. Vlassov, V. V., Giegé, R., and Ebel, J.-P. (1981) *Eur. J. Biochem. 119*, 51−59.
64. Wrede, P., Wurst, R., Vournakis, J., and Rich, A. (1979) *J. Biol. Chem. 254*, 9608−9616.
65. Rhodes, D. (1977) *Eur. J. Biochem. 81*, 91−101.
66. Römer, R., and Hach, R. (1975) *Eur. J. Biochem. 55*, 271−284.
67. Rhodes, D. (1975) *J. Mol. Biol. 94*, 449−460.
68. Prinz, H., Maelicke, A., Cramer, F. (1974) *Biochemistry 13*, 1322−1326.
69. Maglott, E. J., and Glick, G. D. (1997) *Nucleic Acids Res. 25*, 3297−3301.
70. Draper, D. E. (1992) *Acc. Chem. Res. 25*, 201−207.
71. Lynch, D. C., and Schimmel, P. R. (1974) *Biochemistry 13*, 1841−1852.
72. Robison, B., and Zimmerman, T. P. (1971) *J. Biol. Chem. 246*, 110−117.
73. Hyman, E. S. (1980) *Biochim. Biophys. Acta 600*, 553−570.
74. Saenger, W. (1984) *Principles of Nucleic Acid Structure*; pp 331−349, Springer-Verlag, New York.
75. Sprinzl, M., and Gauss, D. H. (1983) in *The Modified Nucleosides of Transfer RNA II* (Agris, P. F., and Kopper, R. A., Eds.) pp 129−226, Alan R. Liss, Inc., New York.
76. Dirheimer, G., Keith, G., Dumas, P., and Westhof, E. (1995) in *tRNA Structure, Biosynthesis, and Function* (Söll, D., and RajBhandary, U. L., Eds.) pp 93−126, ASM Press, Washington, D.C.
77. Yue, D., Kintanar, A., and Horowitz, J. (1994) *Biochemistry 33*, 8905−8911.
78. Pongs, O., and Reinwald, E. (1973) *Biochem. Biophys. Res. Commun. 50*, 357−363.
79. Cameron, V., and Uhlenbeck, O. C. (1973) *Biochem. Biophys. Res. Commun. 50*, 635−640.
80. Krzyzosiak, W. J., and Ciesiolka, J. (1983) *Nucleic Acids Res. 11*, 6913−6921.
81. Davis, D. R., and Poulter, C. D. (1991) *Biochemistry 30*, 4223−4231.
82. Davanloo, P., Sprinzl, M., Watanabe, K., Albani, M., and Kersten, H. (1979) *Nucleic Acids Res. 6*, 1571−1581.
83. Horie, N., Hara-Yokoyama, M., Yokoyama, S., Watanabe, K., Kuchino, Y., Nishimura, S., and Miyazawa, T. (1985) *Biochemistry 24*, 5711−5715.

BI981722U